

Fan-Shaped IIR Filters Based on Analog Prototypes

Radu Matei

Faculty of Electronics, Telecommunications and Information Technology
 “Gheorghe Asachi” Technical University of Iasi, Romania
 rmatei@etti.tuiasi.ro

Abstract—An analytical design method is proposed for 2D IIR fan-shaped filters, using frequency transformations. The design starts from an analog prototype filter with specified parameters and a factored transfer function. Applying adequate frequency transformations, the desired 2D filters are directly obtained in matrix form. The approach is mainly analytical but also uses numerical approximations and is simple, efficient and versatile. Several design examples of fan filters starting from imposed specifications are provided.

Keywords—2D filter design; frequency mapping; image filtering

I. INTRODUCTION

The domain of two-dimensional filters has been studied for at least three decades due to their useful applications in image processing and various approximation and synthesis methods were proposed by many researchers [1], [2]. A fundamental issue regards the spectral transformations, approached in papers like [3], [4]. A currently used design method is based on a 1D prototype filter and transforms its transfer function in order to obtain a 2D filter with a desired frequency response.

There are several types of filters with orientation-selective frequency response, useful in various tasks such as edge detection, motion analysis etc. In [5] a filter bank for directional image decomposition was proposed. A class of linear operators with directional response was introduced in [6]. Wedge filters, named so due to their wedge-like shape in the frequency plane, find applications in feature extraction, e.g. in texture classification [7].

Various design and implementation methods for FIR and IIR fan and wedge filters were introduced in papers like [8]-[13]. Some analytical design methods for 2D fan and wedge filters were proposed by the author in [14]-[16].

Here an analytical design method in the frequency domain for 2D IIR fan-shaped filters is approached, which starts from a given 1D analog prototype filter, whose transfer function is decomposed as a product of elementary functions. Then, a specific frequency transformation is applied, depending on the type of filter to be designed. The design method is based on accurate rational approximations, like Chebyshev-Padé. Since we envisage to design very efficient 2D filters (of minimum order), we will use recursive filters as prototypes, and the 2D fan filters will result recursive as well.

The paper is organized as follows: 1D prototype filters used in design are introduced in section II; the proposed method for fan filter design is described in section III, while several design examples for various parameters are given in section IV.

II. 1D PROTOTYPE FILTERS

An essential step in designing temporal and spatial filters is the approximation. We refer throughout this paper only to recursive spatial filters. Let us consider an analog prototype filter of order N with the transfer function in variable s :

$$H_p(s) = \frac{P(s)}{Q(s)} = \frac{\sum_{i=0}^M p_i \cdot s^i}{\sum_{j=0}^N q_j \cdot s^j} \quad (1)$$

The main issue approached in this paper is to find the transfer function of the desired 2D filter $H_{2D}(z_1, z_2)$ using a complex frequency transformation of the form: $s \rightarrow F(z_1, z_2)$.

In designing a 2D fan-shaped filter we will use a very efficient 1D IIR analog filter prototype. The most efficient analog or digital filter approximation for a specified steepness or selectivity is the elliptic filter, which results of a lower order than other approximations like Butterworth or Chebyshev, for the same specifications. Let us consider next an analog elliptic filter with order $N = 6$, peak-to-peak ripple $R_p = 0.1\text{dB}$, minimum stop-band attenuation $R_s = 36\text{dB}$ and normalized pass-band edge frequency $\omega_p = 0.5$. The specifications given above lead to the following transfer function in the complex frequency variable s :

$$H_p(s) = 0.015849 \cdot \frac{(s^2 + 2.817489)}{(s^2 + 0.564922 \cdot s + 0.131861)} \cdot \frac{(s^2 + 0.505136)}{(s^2 + 0.2223213 \cdot s + 0.225402)} \cdot \frac{(s^2 + 0.347196)}{(s^2 + 0.048334 \cdot s + 0.266546)} \quad (2)$$

Therefore, the 1D elliptic filter transfer function in s given by (2) is factored into three bi-quad functions $H_{B1}(s)$, $H_{B2}(s)$ and $H_{B3}(s)$, each one having the general form:

$$H_{Bi}(s) = \frac{(s^2 + b_0)}{(s^2 + a_1 \cdot s + a_0)} \quad (3)$$

The factors from the numerator and denominator in (2) can be coupled in pairs in several ways. The magnitude of the transfer function (2) is plotted in Fig. 1 on the frequency range $\omega \in [0, \pi]$. By imposing a small value of the pass-band ripple R_p , the low-pass prototype filter is almost maximally-flat but with high steepness, features necessary for the desired 2D fan-shaped filter.

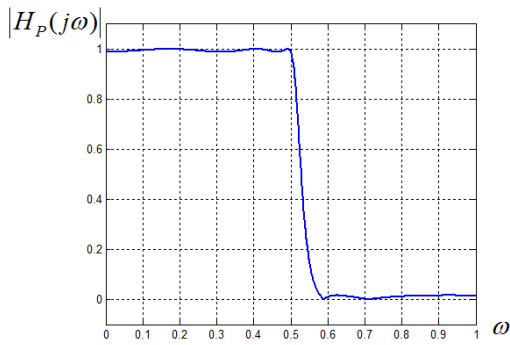


Fig.1 Magnitude of the prototype filter transfer function

III. ANALYTICAL DESIGN METHOD FOR FAN FILTERS

A. Frequency Mapping for Fan-Shaped Filters

In Fig.2 (b) a general fan-type filter is shown, with an aperture angle $\sphericalangle BOD = \theta$, oriented along an axis CC' and its longitudinal axis forming an angle $\sphericalangle AOC = \varphi$ with frequency axis $O\omega_2$. Two particular cases are the two-quadrant fan filter, shown in Fig. 2 (c) and the diagonal fan filter in Fig. 2 (d). Fig. 3 shows a directional filter bank with 8-band frequency partition [5], an angularly-oriented image decomposition which splits the frequency plane into fan-shaped sub-bands.

The 1D analog LP filter discussed in section II will be used as a prototype. The general fan filter can be derived from a LP prototype using the frequency mapping [14]:

$$\omega \rightarrow f_\varphi(\omega_1, \omega_2) = \frac{a \cdot (\omega_1 \cdot \cos \varphi - \omega_2 \cdot \sin \varphi)}{(\omega_1 \cdot \sin \varphi + \omega_2 \cdot \cos \varphi)} \quad (4)$$

In (4), a is the aperture coefficient, given by $a = 1/\text{tg}(\theta/2)$,

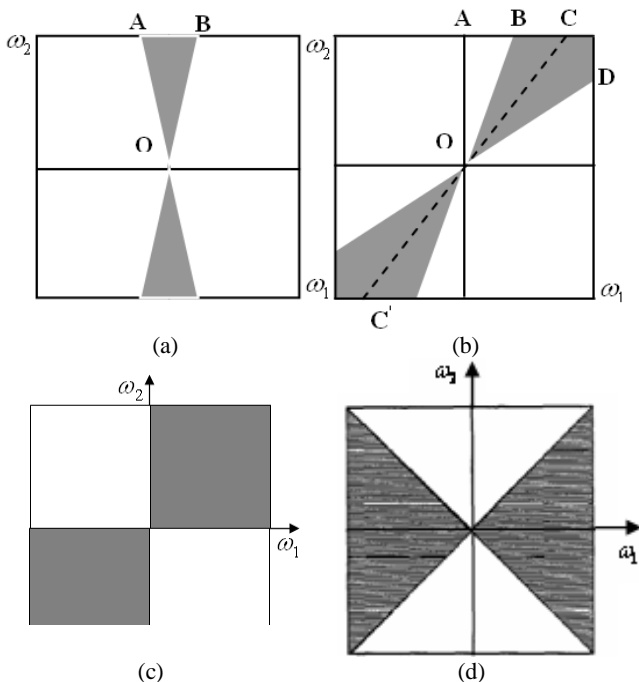


Fig.2. Ideal fan-type filters specified in the frequency plane: (a) along the axis ω_2 ; (b) oriented at an angle φ ; (c) two-quadrant filter; (d) diagonal fan filter

where θ is the aperture angle of the fan filter, as shown in Fig. 2 (b). This frequency mapping can be written in the complex frequency variables $s_1 = j\omega_1$ and $s_2 = j\omega_2$:

$$s \rightarrow f_\varphi(s_1, s_2) = \frac{ja \cdot (s_1 \cdot \cos \varphi - s_2 \cdot \sin \varphi)}{(s_1 \cdot \sin \varphi + s_2 \cdot \cos \varphi)} \quad (5)$$

To find an efficient rational trigonometric approximation of the linear function ω on the range $[-\pi, \pi]$ the simple change of variable is applied:

$$\omega = \arccos(x/\pi) \leftrightarrow x = \pi \cos \omega \quad (6)$$

We first find a trigonometric approximation for the function $\omega/\sin \omega$, using the change of variable (6). Thus, we obtain the first-order Chebyshev-Padé approximation in variable x :

$$\frac{\arccos(x/\pi)}{\sin(\arccos(x/\pi))} = \frac{\arccos(x/\pi)}{\sqrt{1-(x/\pi)^2}} \cong \frac{1.553415 + 0.1099316x}{1 + 0.276857x} \quad (7)$$

Substituting back in (7) $x = \pi \cos \omega$, we get the approximation shown in Fig. 4 (a):

$$\omega \cong 0.39707 \cdot \frac{\sin \omega \cdot (\cos \omega + 4.500234)}{(\cos \omega + 1.150309)} \quad (8)$$

This trigonometric approximation of the linear function is very accurate for $\omega \in [-\pi, \pi]$, with errors only close to the interval margins, where the approximation diverges visibly. Since $\cos \omega = 0.5 \cdot (z + z^{-1})$, we have for ω_1 and ω_2 :

$$\omega_{1,2} \cong \frac{0.39707}{2j} \cdot \frac{(z_{1,2}^2 - z_{1,2}^{-2} + 9.000468 \cdot (z_{1,2} - z_{1,2}^{-1}))}{(z_{1,2} - z_{1,2}^{-1} + 2.300618)} \quad (9)$$

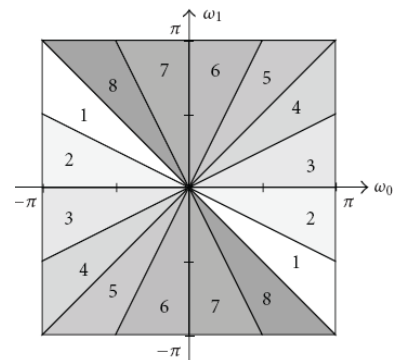


Fig.3. Eight-band partition of the frequency plane

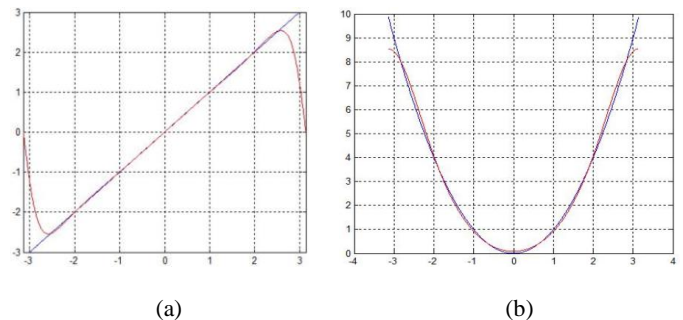


Fig.4 . (a) the approximation (in red) of the linear function (in blue) on the frequency range $\omega \in [-\pi, \pi]$; (b) the parabolic function (in blue) and its rational trigonometric approximation (in red)

For the squared frequency variable we use the following rational trigonometric approximation:

$$\omega^2 \cong 2.357534 \cdot \frac{(1 - 0.946216 \cdot \cos \omega)}{(1 + 0.463012 \cdot \cos \omega)} \quad (10)$$

displayed in Fig. 4 (b). As can be noticed, both are very efficient and accurate approximations on the frequency range $\omega \in [-\pi, \pi]$, having a small distortions only at the margins of the specified interval.

The following step is to substitute the approximation (9) into the frequency mapping (5), separately for the two frequency variables, ω_1 and ω_2 . After some calculations, the mapping with the expression $s \rightarrow f(z_1, z_2)$ may be written in the matrix form:

$$s \rightarrow j \cdot a \cdot f(z_1, z_2) = j \cdot a \cdot \frac{P(z_1, z_2)}{Q(z_1, z_2)} = j \cdot a \cdot \frac{\mathbf{z}_1 \times \mathbf{P} \times \mathbf{z}_2^T}{\mathbf{z}_1 \times \mathbf{Q} \times \mathbf{z}_2^T} \quad (11)$$

where the vectors are:

$$\mathbf{z}_1 = [z_1^4 \quad z_1^3 \quad z_1^2 \quad z_1 \quad 1], \quad \mathbf{z}_2 = [z_2^4 \quad z_2^3 \quad z_2^2 \quad z_2 \quad 1]$$

and the 5×5 matrices \mathbf{P} and \mathbf{Q} can be expressed as:

$$\begin{aligned} \mathbf{P} &= \sin \varphi \cdot \mathbf{M} + \cos \varphi \cdot \mathbf{M}^{90} \\ \mathbf{Q} &= \cos \varphi \cdot \mathbf{M} + \sin \varphi \cdot \mathbf{M}^T \end{aligned} \quad (12)$$

where the superscript T stands for matrix *transposition* and the superscript 90 denotes clockwise matrix rotation with 90 degrees. The 5×5 matrix \mathbf{M} is given by:

$$\mathbf{M} = \begin{bmatrix} 0 & 0 & 0 & 0 & 0 \\ -0.25 & -2.250117 & 0 & 2.250117 & 0.25 \\ -0.575154 & -5.176667 & 0 & 5.176667 & 0.575154 \\ -0.25 & -2.250117 & 0 & 2.250117 & 0.25 \\ 0 & 0 & 0 & 0 & 0 \end{bmatrix} \quad (13)$$

and it is centrally anti-symmetric.

The numerator $P(z_1, z_2)$ and the denominator $Q(z_1, z_2)$ are in fact the Discrete Space Fourier Transforms (DSFT) of the corresponding matrices \mathbf{P} and \mathbf{Q} .

The next step is to substitute the complex mapping (11) into each one of the factors (3) of the analog filter transfer function $H_P(s)$ from (2). Substituting the 1D to 2D mapping (11) into (3), we find the factor $H_{2Bi}(z_1, z_2)$ corresponding to the generic bi-quad function $H_{Bi}(z)$:

$$H_{Bi}(z) \rightarrow H_{2Bi}(z_1, z_2) = \frac{B_i(z_1, z_2)}{A_i(z_1, z_2)} = \frac{\mathbf{z}_1 \times \mathbf{B}_i \times \mathbf{z}_2^T}{\mathbf{z}_1 \times \mathbf{A}_i \times \mathbf{z}_2^T} \quad (14)$$

where \times means inner product and the matrices \mathbf{B}_i and \mathbf{A}_i are given by:

$$\begin{aligned} \mathbf{B}_i &= -a^2 \cdot \mathbf{P} * \mathbf{P} + b_0 \cdot \mathbf{Q} * \mathbf{Q} \\ \mathbf{A}_i &= -a^2 \cdot \mathbf{P} * \mathbf{P} + a_0 \cdot \mathbf{Q} * \mathbf{Q} + j \cdot a \cdot a_1 \cdot \mathbf{P} * \mathbf{Q} \end{aligned} \quad (15)$$

while the vectors \mathbf{z}_1 and \mathbf{z}_2 are: $\mathbf{z}_1 = [z_1^8 \quad z_1^7 \quad \dots \quad z_1 \quad 1]$, $\mathbf{z}_2 = [z_2^8 \quad z_2^7 \quad \dots \quad z_2 \quad 1]$.

To summarize the design method, for a specified orientation φ and an aperture angle θ of the desired fan-shaped filter, the

matrices \mathbf{P} and \mathbf{Q} are determined according to (12). Depending on the filter selectivity, a suitable 1D LP analog prototype is chosen, for instance given by $H_P(s)$ from (2). As the following design examples show, an order $N = 6$ is sufficient for a very good selectivity or steepness. Each bi-quad factor function $H_{Bi}(s)$ of the factored prototype $H_P(s)$ is then simply mapped into $H_{2Bi}(z_1, z_2)$ according to (14). The numerator and denominator of $H_{2Bi}(z_1, z_2)$ correspond to matrices \mathbf{B}_i and \mathbf{A}_i given by (15). The entire 2D filter will have the transfer function given by the product of bi-quads:

$$H_D(z_1, z_2) = \prod_{i=1}^3 H_{2Bi}(z_1, z_2) \quad (16)$$

As the following design examples will show, the resulting 2D filters are quite efficient, i.e. of relatively low order for the imposed performances.

B. Correction Filters

For this class of fan-shaped 2D filters we may need to remove some marginal distortions of the 2D filter frequency response by using a wide band LP filter which has the role of a masking filter applied over the frequency response resulted directly from the design process; this means that the transfer functions of the resulted filter and mask filter are multiplied to obtain the transfer function of the corrected fan filter. We will use two types of zero-phase correction filters which are very easy to design. One of them can be scaled along the two frequency axes of the frequency plane.

A very simple zero-phase LP correction filter results from the function:

$$H_{PC1}(\omega) = \frac{1 + \cos \omega}{1 + p + \cos \omega} \quad (17)$$

where the parameter p gives the steepness (usually $p \ll 1$). This LP filter function is plotted in Fig.5 (a) for three values of the parameter p : 0.01 (red), 0.001 (magenta) and 0.0001 (blue).

A wide square-shaped correction filter simply results by applying the 1D filter (17) along the two frequency plane axes, which is equivalent to the 2D separable filter given by:

$$\begin{aligned} H_{C1}(\omega_1, \omega_2) &= H_{PC1}(\omega_1) \cdot H_{PC1}(\omega_2) \\ &= \frac{(1 + \cos \omega_1) \cdot (1 + \cos \omega_2)}{(1 + p + \cos \omega_1) \cdot (1 + p + \cos \omega_2)} \end{aligned} \quad (18)$$

The function $H_{C1}(\omega_1, \omega_2)$ can also be expressed as a discrete transfer function in z_1 and z_2 .

$$\begin{aligned} H_{C1}(z_1, z_2) &= H_{PC1}(z_1) \cdot H_{PC1}(z_2) \\ &= \frac{(z_1 + 1)^2}{(z_1^2 + 2(1 + p)z_1 + 1)} \cdot \frac{(z_2 + 1)^2}{(z_2^2 + 2(1 + p)z_2 + 1)} \end{aligned} \quad (19)$$

and its magnitude is displayed in Fig. 5 (c) for the parameter value $p = 0.001$.

The second correction filter can be determined from the simple smooth function of frequency with a low-pass shape:

$$H_{PC}(\omega) = 0.5(\tanh(10 \cdot (\omega + 3\pi/4)) - \tanh(10 \cdot (\omega - 3\pi/4))) \quad (20)$$

Using the Chebyshev-Padé expansion, the following rational approximation of $H_{PC}(\omega)$ is obtained:

$$H_{PC2}(\omega) = 1.691967 \cdot \frac{(q^2 \omega^2 - 6.65275)}{(q^2 \omega^2 - 25.492071)} \cdot \frac{(q^2 \omega^2 - 8.230488)(q^2 \omega^2 - 9.598568)}{(q^4 \omega^4 - 11.478865 \cdot q^2 \omega^2 + 34.824872)} \quad (21)$$

This can be regarded as a zero-phase LP filter with a cut-off frequency $3\pi/4$ and is adjustable along the frequency axis through the parameter q . For $q=1$, $H_{PC2}(\omega)$ is a very accurate approximation of $H_{PC}(\omega)$. Fig.5 (b) shows the function $H_{PC}(\omega)$ drawn in red and $H_{PC2}(\omega)$ in blue. In order to find a discrete version of the function (21) we apply the approximation (10) for ω^2 . Substituting (10) in each one of the factors of (21), we obtain a function in variable $\cos \omega$. Since $\cos \omega = 0.5 \cdot (z + z^{-1})$, we get a factored transfer function in variable z , expressed in matrix form like:

$$H_C(z) = \frac{B_C(z)}{A_C(z)} = \frac{\mathbf{B}_C \times \mathbf{z}}{\mathbf{A}_C \times \mathbf{z}} \quad (22)$$

where the vector is $\mathbf{z} = [z^6 \quad z^5 \quad \dots \quad z \quad 1]$, while \mathbf{B}_C and \mathbf{A}_C are vectors of size 1×7 which in turn can be written as convolution of 1×3 and 1×5 vectors as:

$$\mathbf{B}_C = \mathbf{B}_{C1} * \mathbf{B}_{C2} * \mathbf{B}_{C3} \text{ and } \mathbf{A}_C = \mathbf{A}_{C1} * \mathbf{A}_{C2} \text{ where}$$

$$\mathbf{B}_{C1} = [a_1 \quad b_1 \quad a_1], \mathbf{B}_{C2} = [a_2 \quad b_2 \quad a_2],$$

$$\mathbf{B}_{C3} = [a_3 \quad b_3 \quad a_3], \mathbf{A}_{C1} = [a_4 \quad b_4 \quad a_4],$$

$\mathbf{A}_{C2} = [a \quad b \quad c \quad b \quad a]$ and the vector elements have the expressions depending on parameter q :

$$a_1 = -1.115368 \cdot q^2 - 1.540152$$

$$b_1 = 2.357534 \cdot q^2 - 6.65275$$

$$a_2 = -1.115368 \cdot q^2 - 1.905407$$

$$b_2 = 2.357534 \cdot q^2 - 8.230488$$

$$a_3 = -1.115368 \cdot q^2 - 2.222126$$

$$b_3 = 2.357534 \cdot q^2 - 9.598568$$

$$a_4 = -1.115368 \cdot q^2 - 5.901567$$

$$b_4 = 2.357534 \cdot q^2 - 25.492071$$

$$a = 1.244046 \cdot q^4 + 2.964008 \cdot q^2 + 1.86644$$

$$b = -5.259037 \cdot q^4 + 6.538189 \cdot q^2 + 16.124333$$

$$c = 8.046059 \cdot q^4 - 21.133797 \cdot q^2 + 38.557752$$

Once known the 1D transfer function $H_C(z)$, the final transfer function of the 2D square-shaped correction filter

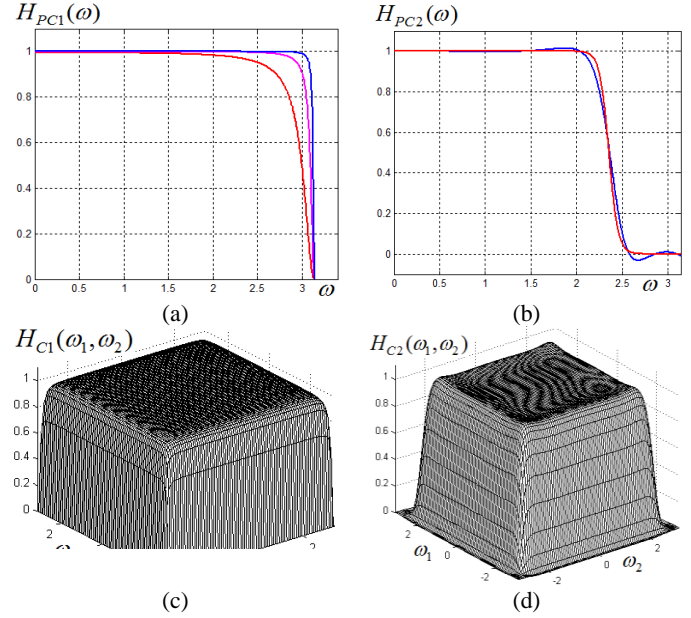


Fig. 5 . (a), (b) Prototype functions for correction filters ; (c), (d) corresponding wide square-shaped correction filters

results as $H_{C2}(z_1, z_2) = H_C(z_1) \cdot H_C(z_2)$. This 2D LP filter is separable and results by applying successively the 1D filter along the two frequency axes. This correction filter is zero-phase and almost maximally-flat, as required. Its characteristic $H_{C2}(\omega_1, \omega_2)$ is displayed in Fig.5 (d).

IV. DESIGN EXAMPLES

Some typical fan filter design examples will be presented in order to illustrate the efficiency of the proposed design method. Let us first consider a two-quadrant filter like in Fig. 2 (c), which is a particular case of a fan filter with orientation angle $\varphi = \pi/4$ and aperture angle $\theta = \pi/2$. The filter frequency response is shown in Fig. 6 (a). While the filter shape is correct and its characteristic is almost maximally-flat, we notice some marginal distortions which are probably due to the marginal approximation error of the linear function, visible in Fig.4 (a). In this case we can apply the first, simpler correction filter given by the function (18) and we obtain the corrected filter whose frequency response magnitude and contour plot are displayed in Fig. 6 (b), (c). In Fig. 6 (d), the uncorrected characteristic of a fan filter like in Fig. 2 (d), with $\varphi = \pi/2$ and $\theta = \pi/2$ is shown. Applying now the second correction filter with parameter $q = 0.9$, we obtain the corrected fan filter shown in Fig. 6 (e) and (f).

The frequency response magnitudes and contour plots of other fan filters are given in Fig. 6 (g), (h) and Fig. 7 (a)-(h), for the specified orientation φ and aperture θ . The filters $H_{F3C}(\omega_1, \omega_2)$ from Fig.6 (g), (h) and $H_{F6C}(\omega_1, \omega_2)$ shown in Fig.7 (e), (f) can be regarded as the components 6 and 5, respectively, of the 8-band partition of the frequency plane shown in Fig.3. Thus, this method allows to design in an analytical manner the components of a directional filter bank,

useful in pattern classification tasks and other image processing operations.

The stability of the designed fan filters was not approached here, but it will be studied in detail in further work on this topic. Generally the stability problem for 2D filters, especially non-separable, is a lot more difficult than for 1D filters. If the prototype filter is stable and if the applied frequency mappings preserve stability, the derived 2D filters should also be stable.

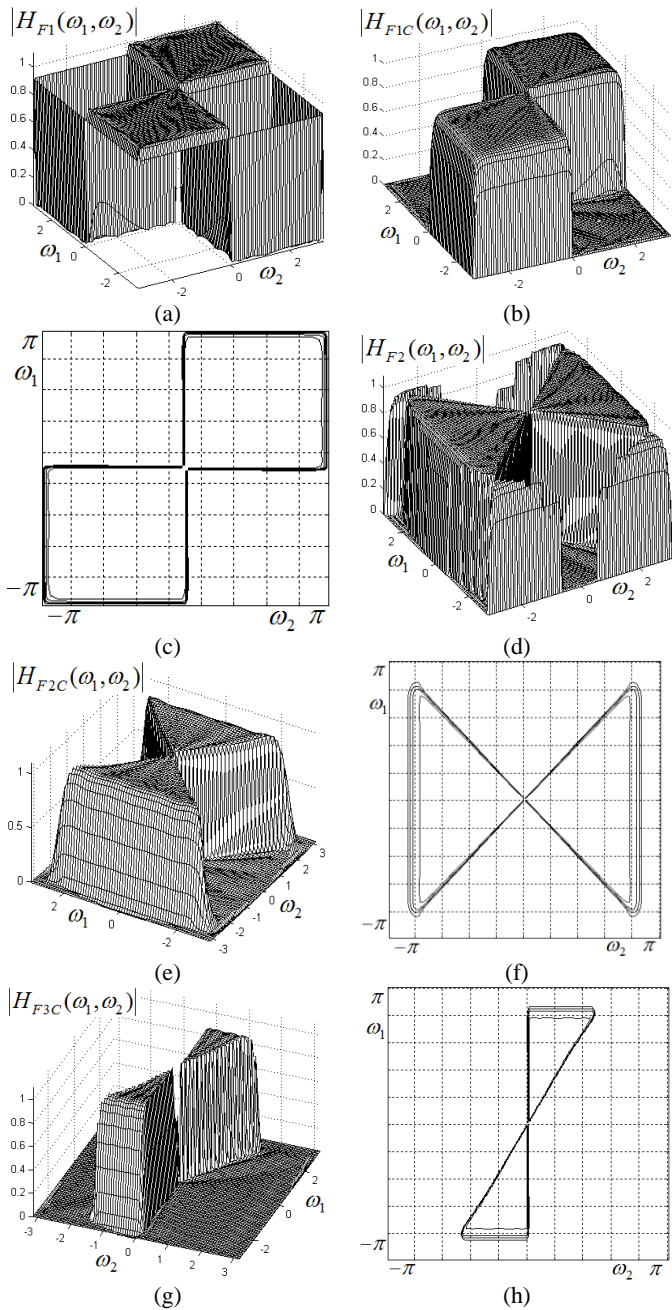


Fig.6. (a) Two-quadrant filter characteristic; (b) corrected characteristic using the simple $H_{C1}(\omega_1, \omega_2)$ filter with $p = 0.001$; (c) contour plot ; (d) fan filter characteristic with $\varphi = \pi/2$, $\theta = \pi/2$; (e), (f) corrected frequency response and contour plot; (g), (h) fan filter with $\varphi = \pi/12$, $\theta = 0.3\pi$;

In the case of an analytical design method for recursive filters like the one proposed here, where the 2D filter transfer function results from its prototype through successive approximations and frequency mappings, stability conditions are difficult to impose from the start. There are however in the literature various stability criteria [17] and also stabilization methods can be applied for unstable 2D filters [18].

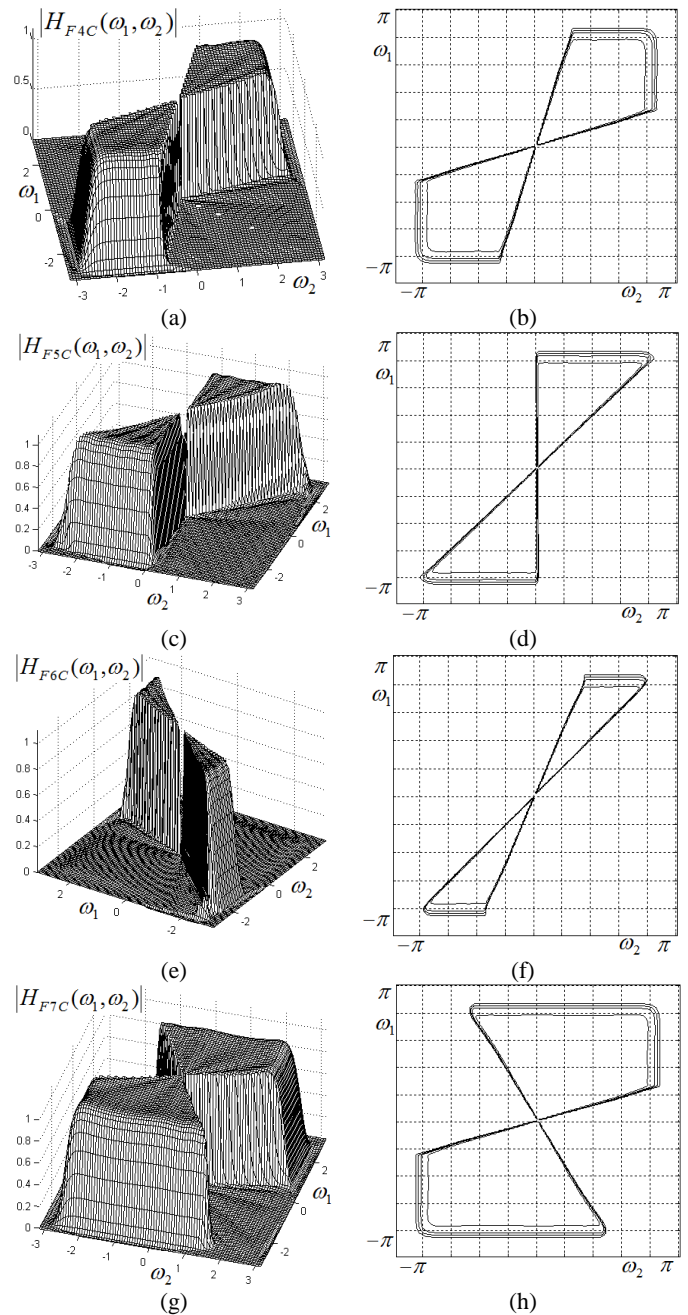


Fig.7. Corrected frequency response magnitudes and contour plots for fan filters with parameters: (a), (b) $\varphi = \pi/4$, $\theta = \pi/4$; (c), (d) $\varphi = \pi/8$, $\theta = 0.44\pi$; (e), (f) $\varphi = 3\pi/16$, $\theta = 0.22\pi$; (g), (h) $\varphi = 0.3\pi$, $\theta = 3\pi/4$

As already mentioned, a set of fan-shaped filters (also named wedge filters, especially for narrower aperture angles) with specified parameter values can be regarded as components of a directional filter bank as the one shown in Fig. 3. Such filter banks are used in applications such as pattern classification and recognition tasks. Such narrow fan or wedge filters are in fact directional filters and can be used in selecting lines with a given orientation from an image. For instance, such filter banks may be applied in medical image analysis, like detection of blood vessels with specified orientation, as shown on some angiography images in [15]. Since such applications are rather well known, simulation results on images were not included in this paper, as the results would be practically similar or comparable with others found in the literature. The purpose of this work was mainly to describe this analytical design technique, to provide design examples and to prove its advantages over an entirely numerical optimization method.

V. CONCLUSION

An analytical design method was proposed for obtaining fan-shaped filters with imposed specifications from a low-pass analog prototype filter. A complex 1D to 2D frequency transformation was derived, which is applied to the analog prototype transfer function and the desired fan-shaped filter results directly in a matrix form. Since the applied mapping is accurate, the resulted 2D filter preserves the characteristics of its prototype, being almost maximally-flat and having a good selectivity, at a relatively low order. The major advantage is the fact that the obtained filter is parametric, in the sense that the specified parameters (aperture and orientation) occur in the 2D filter transfer function. Thus, once known these parameters, the 2D filter is already determined. The design need not be re-made every time for various specifications, as in the case of optimization algorithms.

REFERENCES

- [1] J. S. Lim, *Two-Dimensional Signal and Image Processing*, Prentice-Hall 1990
- [2] W.S. Lu, A. Antoniou, *Two-Dimensional Digital Filters*, CRC Press, 1992
- [3] N.A. Pendergrass, S.K. Mitra, E.I. Jury, *Spectral Transformations for Two-Dimensional Digital Filters*, IEEE Transactions on Circuits and Systems, CAS-23, pp.26-35
- [4] L. Harn, B.A. Shenoi, *Design of Stable Two-Dimensional IIR Filters Using Digital Spectral Transformations*, IEEE Transactions on Circuits and Systems, vol.CAS-33, pp.483-490, May 1986
- [5] R.H. Bamberger, M.J.T. Smith, *A Filter Bank for the Directional Decomposition of Images: Theory and Design*, IEEE Transactions on Signal Processing, Vol. 40 pp. 882-893
- [6] P.E. Danielsson, *Rotation-Invariant Linear Operators With Directional Response*, 5th Int. Conference on Pattern Recognition, Miami, December, 1980
- [7] J.M. Coggins, A.K. Jain, *A Spatial Filtering Approach to Texture Analysis*, Pattern Recognition Letters, Vol.3 (3), 1985
- [8] R. Ansari, *Efficient IIR and FIR Fan Filters*, IEEE Transactions on Circuits and Systems, Vol.34 (8), Aug. 1987, pp.941-945
- [9] Z. Weiping, S. Nakamura, *An Efficient Approach for the Synthesis of 2-D Recursive Fan Filters Using 1-D Prototypes*, IEEE Trans. Signal Processing, Vol.44(4), pp.979-983, Apr. 1996
- [10] G. Qunshan, M.N.S. Swamy, *On the Design of a Broad Class of 2D Recursive Digital Filters with Fan, Diamond and Elliptically-Symmetric Responses*, IEEE Transactions on Circuits and Systems II, Vol.41(9), Sep.1994, pp.603-614

- [11] G.S. Mollova, *Analytical Least Squares Design of 2-D Fan Type FIR Filter*, International Conference on Digital Signal Processing 1997, Vol.2, pp. 625-628
- [12] T.Q. Hung, H.D. Tuan, T.Q. Nguyen, *Design of Half-Band Diamond and Fan Filters by SDP*, IEEE International Conference on Acoustics, Speech and Signal Processing ICASSP 2007, Honolulu, 15-20 April 2007, Vol III, pp. 901 - 904
- [13] A.H. Kayran, R.A. King, *Design of Recursive and Nonrecursive Fan Filters With Complex Transformations*, IEEE Trans. on Circuits and Systems, CAS-30 (12), 1983, pp.849 - 857
- [14] R. Matei, *Design Method for Wedge-Shaped Filters*, Proceedings of the International Conference SIGMAP 2009, Milano, Italy, pp. 19-23
- [15] R.Matei, D.Matei, *Vascular Image Processing Using Recursive Directional Filters*, World Congress on Medical Physics and Biomedical Engineering, Beijing, China, May 26-31, 2012, IFMBE Proceedings Vol. 39 (Springer series), pp. 947-950, ISBN: 978-3-642-29304-7
- [16] R. Matei, *Design Approach for 2D Recursive Filters Used in Frequency Plane Partitioning*, Journal of Scientific Research & Reports (Science Domain International), 12 (4): 1-9, 2016, ISSN 2320-0227
- [17] B.T. O'Connor, T.S. Huang, *Stability of general two-dimensional recursive digital filters*. IEEE Transactions on Acoustics, Speech and Signal Processing, 1978, 26 (6): 550-560
- [18] N. Damera-Venkata, M. Venkataraman, M.S. Hrishikesh, P.S. Reddy, *Stabilization of 2-D recursive digital filters by the DHT method*. IEEE Transactions on Circuits and Systems II, 1999, 46 (1): 85-88, DOI: 10.1109/82.749104